THE JOURNAL OF PHYSICAL CHEMISTRY A

ARTICLE

pubs.acs.org/JPCA

Importance of the Intermolecular Pauli Repulsion in Embedding Calculations for Molecular Properties: The Case of Excitation Energies for a Chromophore in Hydrogen-Bonded Environments

Georgios Fradelos and Tomasz A. Wesołowski*

Département de Chimie Physique, Université de Genève, 30, quai Ernest-Ansermet, CH-1211 Genève 4, Switzerland

Supporting Information

ABSTRACT: In embedding methods such as those labeled commonly as QM/MM, the embedding operator is frequently approximated by the electrostatic potential generated by nuclei and electrons in the environment. Such approximation is especially useful in studies of the potential energy surface of embedded species. The effect on energy of neglecting the non-Coulombic component of the embedding operator is corrected a posteriori. The present work investigates applicability of such approximation in evaluation of electronic excitation energy, the accuracy of which depends directly on that of the embedding potential. For several model systems involving *cis*-7-hydroxiquinoline hydrogen-bonded to small molecules, we demonstrate that such truncation of the embedding operator leads to numerically unstable results upon increasing the size of the atomic basis sets. Approximating the non-Coulombic component of the embedding potential using the expression derived in Frozen-Density Embedding Theory ([Wesolowski and Warshel, *J. Phys. Chem.* **1993**, *97*, 8050] and subsequent works) by means of even a simple bifunctional dependent on the electron density of the chromophore and its hydrogen-bonded environment, restores the numerical stability of the excitation energies that reach a physically meaningful limit for large basis sets.

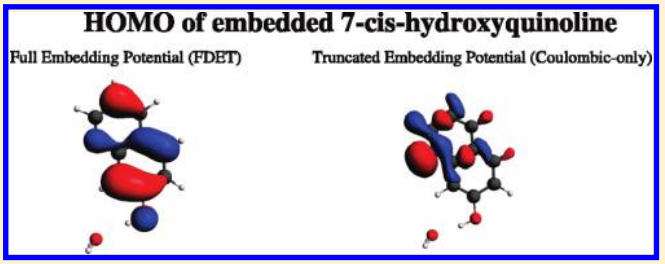

INTRODUCTION

Embedding methods are commonly used in numerical simulations for large polyatomic systems such as biomolecules, materials, solvated molecules, etc. In the case of the Schrödinger equation in Born−Oppenheimer approximation, the principal idea behind the embedding strategy consists of simplifying the basic descriptor of the system: from the N^{tot}-electron function ($\Psi^{N_{tot}}$) to a simpler object - the N^A-electron function (Ψ^{N_A}) where $N_A < N_{tot}$. We will refer to such Ψ^{N_A} as *embedded wave function* (Ψ_{emb}). If N^A denotes the number of electrons of the embedded system in the absence of any environment and $\hat{H}_0$ is the corresponding Hamiltonian, Ψ_{emb} is obtained by solving the following equation:[1]

$$(\hat{H}_0 + \hat{V}_{\mathrm{emb}})\Psi_{\mathrm{emb}} = E_{\mathrm{emb}}\Psi_{\mathrm{emb}} \quad (1)$$

where $\hat{V}_{\mathrm{emb}}$ is an operator representing the effect of the environment on the embedded wave function (embedding operator). Many method are used in practice differing in the strategy to construct $\hat{V}_{\mathrm{emb}}$. By construction, embedding methods must involve subjective choice of the system into its component. If $N_A \ll N_{tot}$, the computational efforts needed to solve eq 1 is significantly smaller than that needed to solve the corresponding Schrödinger equation for the whole system:

$$\hat{H}_{\mathrm{tot}}\Psi^{N_{\mathrm{tot}}} = E_{\mathrm{tot}}\Psi^{N_{\mathrm{tot}}} \quad (2)$$

The embedding methods allow, therefore, for reduction of computational costs without sacrificing accuracy. All quantities evaluated from eq 1 depend on the choice made for the embedding operator and $\hat{H}_o$. In particular, if the environment induced shifts of any evaluated quantity depend critically on the quality of the approximations for the embedding operator.

Frequently, $\hat{V}_{\mathrm{emb}}$ is approximated by means of the electrostatic potential generated by the nuclei in the environment ($v^{\mathrm{B}}_{\mathrm{ext}}(\vec{r})$) and the potential generated by the classical distribution of electrons in the environment (ρ_{B}):

$$v^{\mathrm{eff}}_{\mathrm{emb(coulomb)}}[\rho_{\mathrm{A}},\rho_{\mathrm{B}};\vec{r}] = v^{\mathrm{B}}_{\mathrm{ext}}(\vec{r}) + \int \frac{\rho_{\mathrm{B}}(\vec{r}\,')}{|\vec{r}\,' - \vec{r}|}\mathrm{d}\vec{r}\,' \quad (3)$$

The above generic form of the embedding operator is usually further simplified by using multicenter multipole expansion of the electrostatic potential including (or not) the polarization of the environment by the embedded species. Such potential takes into account the dominant factor influencing the electronic structure of a species embedded in an environment generating strong electrostatic field (ionic solids, polar liquids, for instance) but does not take into account the fermionic statistics of electrons. It is, nevertheless, frequently used. For instance, Shaik et al,[2] write about such

Received: April 6, 2011
Revised: July 14, 2011
Published: July 18, 2011

dx.doi.org/10.1021/jp203192g | *J. Phys. Chem. A* 2011, 115, 10018–10026

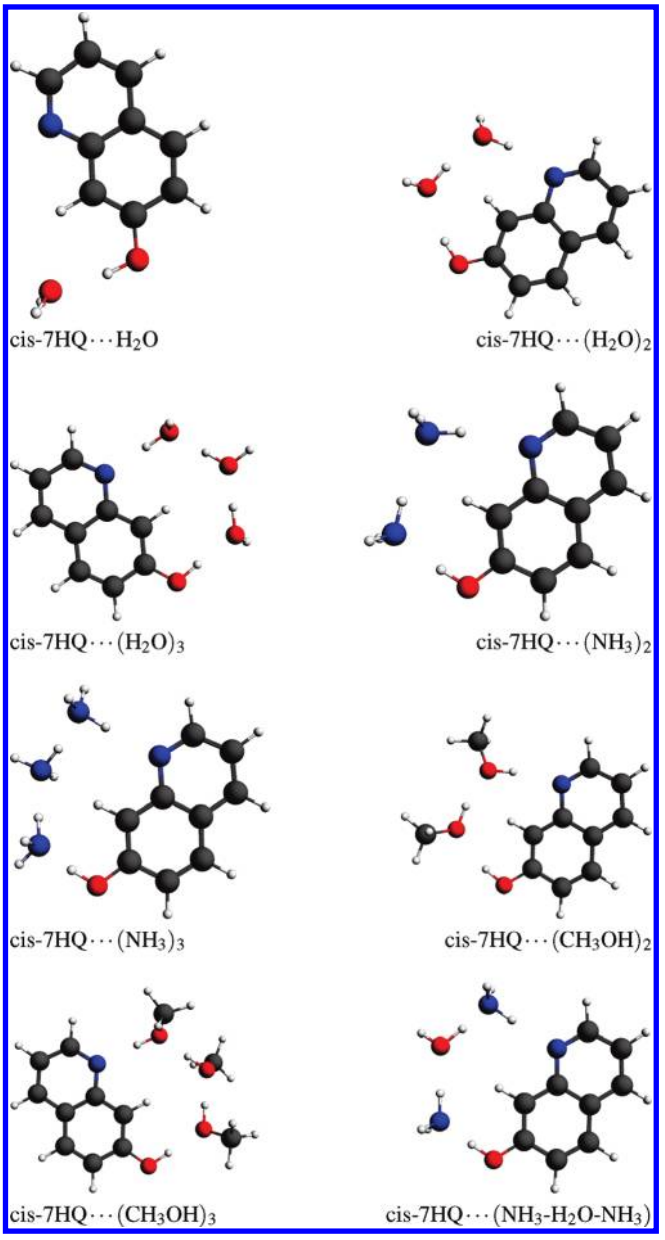

Figure 1. Hydrogen-bonded complexes of the cis-7HQ molecule studied in the present work.

approximation, "Electronic embedding is the standard choice in current QM/MM studies of enzymes.", in the review published last year. Truncating the embedding operator in the electronic Schrödinger equation to its Coulombic component will be referred to as *Coulombic-only approximation* in this work. The Coulombic-only approximation is known to be very adequate in studies targeting the potential energy surface of embedded species as indicated by the aforementioned citation from the review by Shaik et al. and countless reported instances of the QM/MM simulations using the Coulombic-only approximation. The origin of the success of the Coulombic-only approximation lies in the fact that the contributions to the conformational energy resulting from quantum-mechanical origin can be added as a posteriori corrections to the total energy. Such corrections have clear interpretation in the theory of intermolecular interactions and take the form of simple pair potentials which can be derived either from first-principles[3] or involve system-dependent parameters (see the review by Shaik et al.[2] for instance). It is worthwhile to note also that the Coulombic-only approximation is usually applied in combination with highly localized basis sets (see the aforementioned review article by Shaik et al.). When plane waves[4] or basis sets extending to the environment are used,[5,6] flaws of this approximation are revealed that lead to a qualitatively wrong distribution of charge density between the embedded species and the environment. For other observables than the energy, the a posteriori correction of errors resulting from the Coulombic-only approximation is less straightforward. For each observable associated with a given operator other than electronic Hamiltonian, a priori correction would involve parametrizing its expectation value. Several authors clearly indicated the need of going beyond the Coulombic-only approximation and proposed methods in which the Coulombic-only embedding potential is supplemented by either local/nonlocal pseudopotentials or dumping factors for electrostatic interactions[4,7−11] as part of the embedding operator. Despite this accumulated numerical evidence of indispensability of taking into account the non-Coulombic part of the embedding operator, the Coulombic-only approximation is still in use even in simulations targeting excitation energies.[12−19] Interestingly, the reported excitation energies obtained using the Coulombic-only approximations are frequently very good. We attribute this to the use of basis sets localized in the embedded chromophore in such cases. The basis sets used in such calculations do not allow for fully variational exploration of the potential far from the chromophore, that is, where the Coulombic-only approximation is least adequate. The present work provides a systematic analysis of the limits of applicability of the Coulombic-only approximation to the embedding potential and its ability to yield convergent results with increasing size of the basis sets. The *cis*-7-hydroxyquinoline molecule (cis-7HQ) in different environments was chosen for studying this approximation. Eight environments consisting of 1−3 small hydrogen-bonded molecules: water, ammonia, and methanol (see Figure 1) were considered. The structural and spectroscopic properties of the investigated complexes are well understood, owing to spectroscopic data obtained in molecular beams and theoretical calculations.[20]

In both aforementioned strategies to treat non-Coulombic component of the embedding operator involving pseudopotentials or dumping factors, this component is represented in a system-dependent manner. Frozen-Density Embedding Theory (FDET),[21−25] on the other hand, provides a system-independent expression for the non-Coulombic component of the embedding operator expressed as local potential. The system dependency is the result of the fact that this potential is shown to be a bifunctional depending on a pair of electron densities: that of the embedded species (ρ_A) and that of the environment (ρ_B). If $\hat{H}_0$ and Ψ_{emb} define (*i*) the noninteracting reference system (Kohn−Sham case),[21,22] (*ii*) the full Configuration Interaction case,[23] or (*iii*) the system defined by one-particle density matrix,[24] the embedding potential of FDET takes the following form:

$$v_{emb}^{eff}[\rho_A,\rho_B;\vec{r}] = v_{ext}^{B}(\vec{r}) + \int \frac{\rho_B(\vec{r}\,')}{|\vec{r}\,'-\vec{r}|}d\vec{r}\,' + \left.\frac{\delta E_{xc}[\rho]}{\delta\rho}\right|_{\rho=\rho_A+\rho_B} - \left.\frac{\delta E_{xc}[\rho]}{\delta\rho}\right|_{\rho=\rho_A} + \left.\frac{\delta T_s[\rho]}{\delta\rho}\right|_{\rho=\rho_A+\rho_B} - \left.\frac{\delta T_s[\rho]}{\delta\rho}\right|_{\rho=\rho_A} \quad (4)$$

dx.doi.org/10.1021/jp203192g |*J. Phys. Chem. A* 2011, 115, 10018–10026

where the nonadditive bifunctionals are defined as $X^{nad}[\rho_A,\rho_B] = X[\rho_A + \rho_B] - X[\rho_A] - X[\rho_B]$, with $X[\rho]$ denoting the density functional for either the exchange-correlation or noninteracting kinetic energy ($E_{xc}[\rho]$ and $T_s[\rho]$, respectively). Note that the notation used in eq 4, $v^{eff}_{emb}[\rho_A,\rho_B;\vec{r}]$ and not $v^{eff}_{emb}[\rho_A,\rho_B];(\vec{r})$, reflects the fact that the whole FDET embeding potential, opposite to its non-Coulombic components, is not the bifunctional of ρ_A and ρ_B because it comprises the ρ_A,ρ_B independent part ($v^{B}_{ext}(\vec{r})$.

For embedding a system described by an interacting Hamiltonian and the wave function of truncated Configuration Interaction form, the embedding functional comprises also an additional term assuring the self-consistency between energy and embedded wave function which depends on the number of determinants used to construct the embedded wave function.[23] Various computational methods based on FDET differing in (*i*) the approximations for the bifunctional for the non-Coulombic part of the embedding operator, (*ii*) the choice for $\hat{H}_0$, (*iii*) approximation for ρ_B, and (*iv*) additional approximations used in obtaining various observables from the embedded wave function, have been developed by us (see ref 26 for a recent example) and others.[27−33]

The second objective of the study is the analysis of the numerical stability of shifts in the excitation energies derived using the full potential given in eq 4, in which the exact bifunctionals are replaced by their approximate counterparts. The used approximate bifunctionals and the choice for ρ_B in eq 4 were demonstrated to lead to the hydrogen-bonding induced shifts in the considered chromophore, which are equivalent to the results of benchmark wave function based ones (see ref 34). The Coulombic-only approximation can be seen as an even more drastic approximation to the exact embedding potential given in eq 4 in which all nonadditive bifunctionals are simply neglected.

In particular, our own studies showed that the FDET based calculations using the same approximations as the ones applied in the present work provide highly accurate hydrogen-bonding induced shifts of the lowest excitation energies. In a sample of several similar complexes partially overlapping with the ones analyzed in the present work, it was shown that FDET-based shifts are comparable in accuracy to the Equation-of-Motion Coupled Cluster results of the benchmark quality.[34,35] We note also that a similar study on the adequacy for evaluation of the environment induced changes of an other property (*g*-tensor) of both the full potential given in eq 4 and its truncated Coulombic-only approximation was recently reported,[36] where it was shown that taking into account the non-Coulombic component of the embedding operator is indispensable.

COMPUTATIONAL DETAILS

The calculations of the electronic excitations and their shifts follow the general framework of Linear-Response Time-Dependent Density Functional Theory in its original version for the isolated chromophore or its embedding version introduced in ref 5 for the chromophore in the complex. The embedded orbitals and their levels were obtained from the Kohn−Sham Equations for Constrained Electron Density [cf., eqs 20 and 21 in our original work[21]]:

$$\left[-\frac{1}{2}\nabla^2 + v^{eff}_{KS}[\rho_A;\vec{r}] + v^{eff}_{emb}[\rho_A,\rho_B;\vec{r}]\right]\phi^A_i = \varepsilon^A_i\phi^A_i \quad (5)$$

where $v^{eff}_{KS}[\rho_A;\vec{r}]$ is the usual expression for the potential of the Kohn−Sham DFT for the isolated system A, where A refers to the chromophore, whereas B refers to the environment throughout the present work. For each case, the Kohn−Sham ground-state electron density of the molecules in the environment in the absence of the chromophore was used as ρ_B. The excitation energy of the embedded chrompohore was calculated by replacing the Kohn−Sham effective potential in the LR-TDDFT equations[38] by the effective potential in eq 5 evaluated at the same ρ_B. Such treatment of ρ_B defines an additional approximation in LR-TDDFT (neglect of dynamic response of the environment, NDRE approximation in short). The adequacy of NDRE depends on the system under investigation. NDRE cannot be used if the absorption spectra of the embedded species and the molecules in the environment overlap, as comprehensively demonstrated by Neugebauer.[37] The formalism introduced by Casida and Wesolowski[38] generalizing in the ground-state subsystem formulation of DFT[39,40] for excited states, makes it possible to go beyond NDRE. This formalism has not been fully implemented numerically so far. Its simplified version, however, allowing for coupling between selected excitations in different chromophores, was developed by Neugebauer.[37] Because the electronic spectra of the environment molecules and the chromophore are separated, NDRE is applicable here.

The geometries of each complex were obtained using the method based on the subsystem formulation of DFT (the code deMon2k-KSCED,[41] which is based on the code deMon2k[42]) applying local density approximation for all relevant bifunctionals and functionals implemented in the deMon2k code (see ref 43 for details). The geometries are provided in the Supporting Information.

The relevant equations of FDET and its LR-TDDFT[44] extension in NDRE approximation[5] have been originally implemented into ADF code by Wesolowski.[5] The improved implementation[45,46] in the ADF2009.01 version[47] was used in the present work.

The density ρ_B was obtained from Kohn−Sham calculations using the SAOP[48] exchange-correlation potential and the STO-TZ2P basis set (triple-ζ basis with two sets of polarization functions) from the ADF2009.01 database. The following approximations were used in the embedding potential: for the exchange-correlation depended part, the Perdew−Wang (PW91) functional[49] and for the kinetic energy depended part the recently developed NDSD bifunctional,[25] which takes into account the exact conditions that become relevant for the proper behavior of $v^{nad}_t[\rho_A,\rho_B](\vec{r})$ in the vicinity of nuclei, whereas the SAOP potential was used for the exchange-correlation component of $v^{eff}_{KS}[\rho_A;\vec{r}]$ in eq 5.

For the chromophore, the following basis sets defined in the ADF2009.01 database were used: STO-SZ (single-ζ basis), STO-DZ (double-ζ basis), STO-ATZP (triple-ζ basis with one sets of polarization functions and one set of diffuse s-STO and p-STO functions), and STO-ATZP+gh (where gh stands for ghosts and indicates that the STO-ATZP atomic functions were used not only for the atomic centers of the chromophore, but also at atoms in the environment).

Throughout this work, $\Delta\omega$ denotes the environment induced shift in the vertical excitation energy for the lowest excitation cis-7HQ ($\Delta\omega = \omega^{embedded} - \omega^{isolated}$). $\Delta\varepsilon^{HOEO}$ denotes the corresponding shift in the energy of the highest occupied embedded orbital (HOEO) compared to the energy of the highest occupied molecular orbital (HOMO) of the isolated chromophore, $\Delta\varepsilon^{HOEO} = \varepsilon^{HOEO} - \varepsilon^{HOMO}$, and $\Delta\varepsilon^{LUEO}$ denotes the shift of the energy of the lowest unoccupied embedded

Table 1. Basis Set Dependence of the FDET Results for *cis*-7-Hydroxyquinoline Hydrogen Bonded to One H_2O Molecule Obtained with Coulombic-Only (eq 3) and Full (eq 4) Embedding Potentials: Shift of the Lowest Excitation ($\Delta\omega$, in cm^{-1}), Shift of the Highest Occupied Embedded Orbital Energy ($\Delta\varepsilon^{HOEO}$ in eV), and Shift of the Lowest Unoccupied Embedded Orbital Energy ($\Delta\varepsilon^{LUEO}$ in eV)[a]

basis set	$\Delta\omega$	$\Delta\varepsilon^{HOEO}$	$\Delta\varepsilon^{LUEO}$
Coulombic-Only Embedding Potential			
STO-SZ	108	0.225	0.234
STO-DZ	−858	0.434	0.342
STO-ATZP	−12999	0.268	−0.846
STO-ATZP-gh	−29008	−4.429	−7.585
Full Embedding Potential			
STO-SZ	129	0.237	0.248
STO-DZ	−922	0.470	0.371
STO-ATZP	−621	0.348	0.284
STO-ATZP+gh	−658	0.340	0.271

[a] The experimental complexation induced shift of the $S_o \rightarrow S_1$ excitation is -590 cm^{-1}.[20]

Table 2. Basis Set Dependence of the FDET Results for *cis*-7-Hydroxyquinoline Hydrogen Bonded to Two H_2O Molecules Obtained with Coulombic-Only (eq 3) and Full (eq 5) Embedding Potentials: Shift of the Lowest Excitation ($\Delta\omega$, in cm^{-1}), Shift of the Highest Occupied Embedded Orbital Energy ($\Delta\varepsilon^{HOEO}$ in eV), and Shift of the Lowest Unoccupied Embedded Orbital Energy ($\Delta\varepsilon^{LUEO}$ in eV)[a]

basis set	$\Delta\omega$	$\Delta\varepsilon^{HOEO}$	$\Delta\varepsilon^{LUEO}$
Coulombic-Only Embedding Potential			
STO-SZ	2285	0.039	−0.048
STO-DZ	−1710	0.074	−0.114
STO-ATZP	−8535	−0.030	−0.596
STO-ATZP+gh			
Full Embedding Potential			
STO-SZ	2184	0.078	−0.019
STO-DZ	−1703	0.166	−0.022
STO-ATZP	−1626	0.148	−0.026
STO-ATZP+gh	−1629	0.144	−0.030

[a] Unfilled fields denote lack of convergent solutions. The experimental complexation induced shift of the $S_o \rightarrow S_1$ excitation is -1637 cm^{-1}.[20]

orbital (LUEO) compared to the energy of the lowest unoccupied molecular orbital (LUMO) of the isolated chromophore, $\Delta\varepsilon^{LUEO} = \varepsilon^{LUEO} - \varepsilon^{LUMO}$. The shifts of the excitation energies and orbital energies were evaluated as differences of the corresponding quantities evaluated with and without the environment at the unchanged geometry of the chromophore.

RESULTS AND DISCUSSION

We start with the results obtained with the full embedding potential given in eq 4. For cis-7HQ···H_2O, which is the smallest complex investigated here, $\Delta\omega$ changes sign from +129 cm^{-1} to −922 cm^{-1} upon increasing the basis set from

Table 3. Basis Set Dependence of the FDET Results for *cis*-7-Hydroxyquinoline Hydrogen Bonded to Three H_2O Molecules Obtained with Coulombic-Only (eq 3) and Full (eq 5) Embedding Potentials: Shift of the Lowest Excitation ($\Delta\omega$, in cm^{-1}), Shift of the Highest Occupied Embedded Orbital Energy ($\Delta\varepsilon^{HOEO}$ in eV), and Shift of the Lowest Unoccupied Embedded Orbital Energy ($\Delta\varepsilon^{LUEO}$ in eV)[a]

basis set	$\Delta\omega$	$\Delta\varepsilon^{HOEO}$	$\Delta\varepsilon^{LUEO}$
Coulombic-Only Embedding Potential			
STO-SZ	2021	0.070	−0.052
STO-DZ	−1993	0.087	−0.129
STO-ATZP		0.028	−1.742
STO-ATZP+gh	−27319	−16.065	−18.994
Full Embedding Potential			
STO-SZ	1813	0.137	−0.008
STO-DZ	−1938	0.182	−0.030
STO-ATZP	−1769	0.164	−0.024
STO-ATZP+gh	−1811	0.158	−0.035

[a] Unfilled fields denote lack of convergent solutions. The experimental complexation induced shift of the $S_o \rightarrow S_1$ excitation is -2060 cm^{-1}.[20]

STO-SZ to the STO-DZ (see Table 1). The addition of diffused functions to the monomer basis set (STO-ATZP) results in a noticeable effect on the shift reducing it to -621 cm^{-1}. The addition of more centers to the STO-ATZP basis set by including ghosts (STO-ATZP-gh) localized in the environment, which is the H_2O molecule in this case, affect further the shift but the effect is significantly smaller (less than 40 cm^{-1}). Note that the energy of the lowest excitation in isolated cis-7HQ varies within the 80 cm^{-1} range if additional ghost centers carrying the STO-ATZP basis sets are used (see Table 9). Except for the STO-SZ basis set case, the lowest excitation obtained from LR-TDDFT calculations involves mainly the highest occupied and lowest occupied embedded orbitals, each of them being of the π character ($\pi \rightarrow \pi^*$ transition).

The above trends in the dependence of the excitation energy on the basis set are reflected also in the shifts in orbital energies ($\Delta\varepsilon$). $\Delta\varepsilon^{HOEO}$ becomes much more positive when one goes from STO-SZ basis set to the STO-DZ basis set (from 0.237 to 0.470 eV), then much more negative (0.348 eV for STO-ATZP) and finally slightly more negative (0.340 eV) for STO-ATZP+gh. Almost the same pattern is observed for the $\Delta\varepsilon^{LUEO}$. The relative numerical stability of the $\Delta\varepsilon^{HOEO}$ and $\Delta\varepsilon^{LUEO}$ obtained with the larger than STO-SZ basis sets is reflected also in the shape of the frontier orbitals. Figures 4 and 5 show that the shape of the embedded frontier orbitals obtained with the STO-DZ, STO-ATZP, and STO-ATZP+gh basis sets is basically indistinguishable. For the cis-7HQ···$(H_2O)_2$ complex, similar tendencies in the basis set dependency of $\Delta\omega$ and $\Delta\varepsilon^{HOEO}$ occur. The magnitudes of the shifts calculated for each considered basis set are, however, larger, reflecting thus the stronger interactions with the chromophore (two hydrogen bonds linking the chromophore with the environment). The analysis of Tables 1−8 collecting the results for all the complexes investigated in this work reveals several common tendencies in the basis set dependency of the analyzed quantities if obtained with the full embedding potential. The self-consistent procedure to obtain embedded orbitals (solving eq 5) and the Davidson procedure[50] to

Table 4. Basis Set Dependence of the FDET Results for *cis*-7-Hydroxyquinoline Hydrogen Bonded to Two NH_3 Molecules Obtained with Coulombic-Only (eq 3) and Full (eq 5) Embedding Potentials: Shift of the Lowest Excitation ($\Delta\omega$, in cm^{-1}), Shift of the Highest Occupied Embedded Orbital Energy ($\Delta\varepsilon^{HOEO}$ in eV), and Shift of the Lowest Unoccupied Embedded Orbital Energy ($\Delta\varepsilon^{LUEO}$ in eV)[a]

basis set	$\Delta\omega$	$\Delta\varepsilon^{HOEO}$	$\Delta\varepsilon^{LUEO}$
Coulombic-Only Embedding Potential			
STO-SZ	2351	0.295	0.215
STO-DZ	−1554	0.324	0.153
STO-ATZP	−18325	0.142	−1.634
STO-ATZP+gh			
Full Embedding Potential			
STO-SZ	2140	0.365	0.261
STO-DZ	−1609	0.415	0.238
STO-ATZP	−1517	0.399	0.237
STO-ATZP+gh	−1477	0.402	0.243

[a]Unfilled fields denote lack of convergent solutions. The experimental complexation induced shift of the $S_o \rightarrow S_1$ excitation is -1715 cm^{-1}.[20]

Table 5. Basis Set Dependence of the FDET Results for *cis*-7-Hydroxyquinoline Hydrogen Bonded to Three NH_3 Molecules Obtained with Coulombic-Only (eq 3) and Full (eq 5) Embedding Potentials: Shift of the Lowest Excitation ($\Delta\omega$, in cm^{-1}), Shift of the Highest Occupied Embedded Orbital Energy ($\Delta\varepsilon^{HOEO}$ in eV), and Shift of the Lowest Unoccupied Embedded Orbital Energy ($\Delta\varepsilon^{LUEO}$ in eV)[a]

basis set	$\Delta\omega$	$\Delta\varepsilon^{HOEO}$	$\Delta\varepsilon^{LUEO}$
Coulombic-Only Embedding Potential			
STO-SZ	2089	0.351	0.237
STO-DZ	−1791	0.367	0.171
STO-ATZP	−24997	0.189	−2.414
STO-ATZP+gh	−28324	−16.277	−19.342
Full Embedding Potential			
STO-SZ	1824	0.434	0.290
STO-DZ	−1833	0.455	0.253
STO-ATZP	−1681	0.433	0.253
STO-ATZP+gh	−1664	0.440	0.261

[a]Unfilled fields denote lack of convergent solutions. The experimental complexation induced shift of the $S_o \rightarrow S_1$ excitation is -2030 cm^{-1}.[20]

solve the Casida equations[44] always converge (see Tables 1−8). The numerical values of $\Delta\omega$, $\Delta\varepsilon^{HOEO}$, and $\Delta\varepsilon^{LUEO}$ seem to stabilize with the increase of the basis set. In fact, adding the basis sets localized in the environment (making the results prone to any inaccuracies in the embedding potential) results in a very small (usually less than 40 cm^{-1}) numerical effect (see the STO-ATZP or STO-ATZP+gh results collected in Tables 1−8). The good numerical stability of the calculated shifts reflects the variational origin of the applied FDET-based calculations. It is

Table 6. Basis Set Dependence of the FDET Results for *cis*-7-Hydroxyquinoline Hydrogen Bonded to Two CH_3OH Molecules Obtained with Coulombic-Only (eq 3) and Full (eq 5) Embedding Potentials: Shift of the Lowest Excitation ($\Delta\omega$, in cm^{-1}), Shift of the Highest Occupied Embedded Orbital Energy ($\Delta\varepsilon^{HOEO}$ in eV), and Shift of the Lowest Unoccupied Embedded Orbital Energy ($\Delta\varepsilon^{LUEO}$ in eV)[a]

basis set	$\Delta\omega$	$\Delta\varepsilon^{HOEO}$	$\Delta\varepsilon^{LUEO}$
Coulombic-Only Embedding Potential			
STO-SZ	2155	0.111	0.010
STO-DZ	−1824	0.142	−0.058
STO-ATZP	−16291	0.031	−1.456
STO-ATZP+gh	−27053	−22.290	−25.424
Full Embedding Potential			
STO-SZ	2048	0.151	0.040
STO-DZ	−1819	0.235	0.035
STO-ATZP	−1734	0.216	0.031
STO-ATZP+gh	−1727	0.223	0.039

[a]Unfilled fields denote lack of convergent solutions. The experimental complexation induced shift of the $S_o \rightarrow S_1$ excitation is -1868 cm^{-1}.[20]

Table 7. Basis Set Dependence of the FDET Results for *cis*-7-Hydroxyquinoline Hydrogen Bonded to Three CH_3OH Molecules Obtained with Coulombic-Only (eq 3) and Full (eq 5) Embedding Potentials: Shift of the Lowest Excitation ($\Delta\omega$, in cm^{-1}), Shift of the Highest Occupied Embedded Orbital Energy ($\Delta\varepsilon^{HOEO}$ in eV), and Shift of the Lowest Unoccupied Embedded Orbital Energy ($\Delta\varepsilon^{LUEO}$ in eV)[a]

basis set	$\Delta\omega$	$\Delta\varepsilon^{HOEO}$	$\Delta\varepsilon^{LUEO}$
Coulombic-Only Embedding Potential			
STO-SZ	1894	0.137	0.000
STO-DZ	−2114	0.148	−0.082
STO-ATZP			
STO-ATZP+gh			
Full Embedding Potential			
STO-SZ	1670	0.209	0.047
STO-DZ	−2063	0.248	0.021
STO-ATZP	−1890	0.230	0.029
STO-ATZP+gh	−1920	0.226	0.021

[a]Unfilled fields denote lack of convergent solutions. The experimental complexation induced shift of the $S_o \rightarrow S_1$ excitation is -2329 cm^{-1}.[20]

worthwhile to underline that the shifts in the vertical excitation energies obtained with the two largest basis sets considered are in good agreement with the closely related experimental quantities, the complexation induced shifts of the origin of the $S_o \rightarrow S_1$ excitation collected in Table 10.

To investigate the importance of the non-Coulombic component of the orbital-free embedding potential, we turn now our attention to the results obtained with the truncated embedding potential (Coulombic-only embedding). The situation changes qualitatively compared to the discussed previously full potential

Table 8. Basis Set Dependence of the FDET Results for *cis*-7-Hydroxyquinoline Hydrogen Bonded to One H_2O and Two NH_3 Molecules Obtained with Coulombic-Only (eq 3) and Full (eq 5) Embedding Potentials: Shift of the Lowest Excitation ($\Delta\omega$, in cm^{-1}), Shift of the Highest Occupied Embedded Orbital Energy ($\Delta\varepsilon^{HOEO}$ in eV), and Shift of the Lowest Unoccupied Embedded Orbital Energy ($\Delta\varepsilon^{LUEO}$ in eV)[a]

basis set	$\Delta\omega$	$\Delta\varepsilon^{HOEO}$	$\Delta\varepsilon^{LUEO}$
Coulombic-Only Embedding Potential			
STO-SZ	1953	0.326	0.196
STO-DZ	−1964	0.337	0.123
STO-ATZP		0.202	−2.496
STO-ATZP+gh	−28123	−16.203	−19.244
Full Embedding Potential			
STO-SZ	1688	0.409	0.249
STO-DZ	−1991	0.429	0.221
STO-ATZP	−1800	0.404	0.209
STO-ATZP+gh	−1844	0.410	0.216

[a]Unfilled fields denote lack of convergent solutions. The experimental complexation induced shift of the $S_o \rightarrow S_1$ excitation is $-1780\ cm^{-1}$.[20]

Table 9. Lowest Vertical Excitation Energy ω (in cm^{-1}) in Isolated *cis*-7-Hydroxyquinoline, the Energy of the Highest Occupied Orbital ε^{HOMO} (in eV), and the Energy of the Lowest Unoccupied Orbital ε^{LUMO} (in eV) Evaluated with Different Basis Sets in LR-TDDFT Calculations

basis set	ω	ε^{HOMO}	ε^{LUMO}
STO-DZ	29770	−7.404	−3.952
STO-DZ	31633	−10.232	−6.834
STO-ATZP	30700	−9.712	−6.411
STO-ATZP+gh (H_2O)	30709	−9.721	−6.419
STO-ATZP+gh ($(H_2O)_2$)	30722	−9.719	−6.417
STO-ATZP+gh ($(H_2O)_3$)	30632	−9.699	−6.403
STO-ATZP+gh ($(NH_3)_2$)	30737	−9.705	−6.400
STO-ATZP+gh ($(NH_3)_3$)	30742	−9.704	−6.399
STO-ATZP+gh ($(CH_3OH)_2$)	30661	−9.664	−6.368
STO-ATZP+gh ($(CH_3OH)_3$)	30689	−9.679	−6.378
STO-ATZP+gh ($NH_3-H_2O-NH_3$)	30663	−9.687	−6.390

case. The shifts collected in Tables 1−8 seem to depend strongly on the basis set. Let us start with the complex cis-7HQ···(H_2O) and the results obtained with the two smallest basis sets (STO-SZ and STO-DZ). For STO-SZ, similarly as in the previously discussed full-potential case, not the lowest but the second-lowest transition obtained from LR-TDDFT calculations has the $\pi \rightarrow \pi^*$ character. For STO-DZ, similarly as in full potential calculations the lowest excitation is, indeed, a $\pi \rightarrow \pi^*$ transition. The shifts in the excitation energies calculated with the full and with the truncated (Coulombic-only) embedding potential agree quite reasonably (see Table 1) of the smallest basis sets are used. The increase of the basis set from STO-SZ to STO-DZ affects the results obtained with these two potentials in a similar way. For instance, $\Delta\omega$ also changes sign from +108 to $-858\ cm^{-1}$ (the

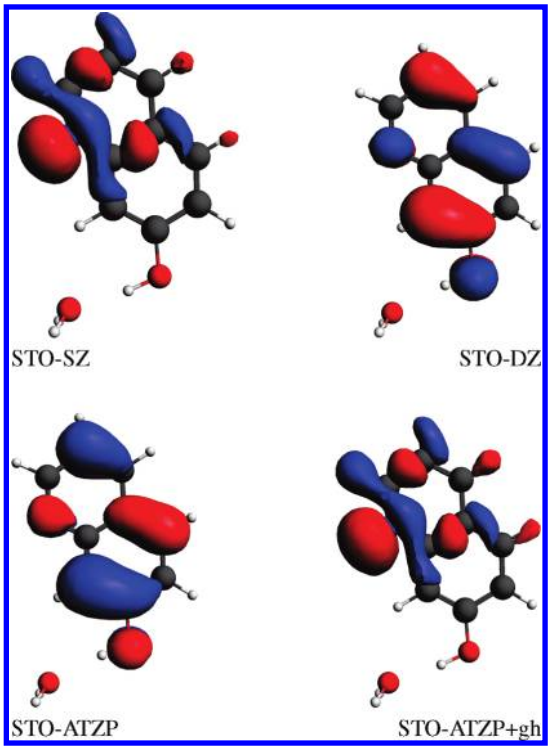

Figure 2. Highest occupied embedded orbital obtained with different basis sets and the Coulombic-only embedding potential: the cis-7HQ-H_2O case.

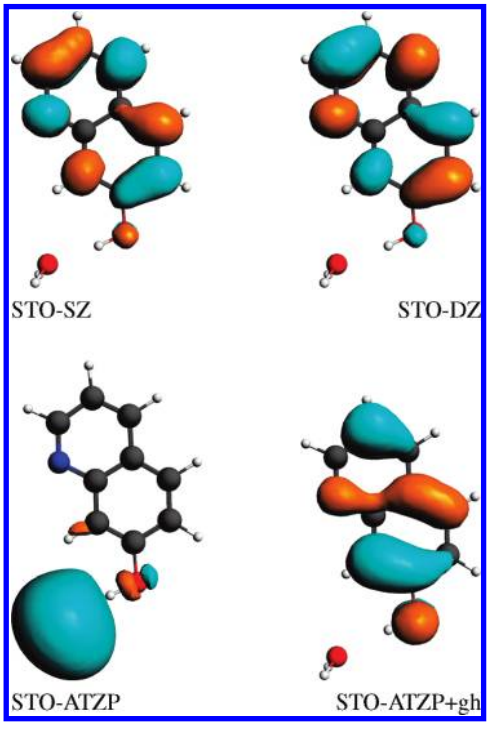

Figure 3. Lowest unoccupied embedded orbital obtained with different basis sets and the Coulombic-only embedding potential: the cis-7HQ-H_2O case.

corresponding full embedding potential results are 129 and $-922\ cm^{-1}$), $\Delta\varepsilon^{HOEO}$ becomes much more positive and increases from 0.225 to 0.434 eV (the corresponding full potential

dx.doi.org/10.1021/jp203192g |J. Phys. Chem. A 2011, 115, 10018–10026

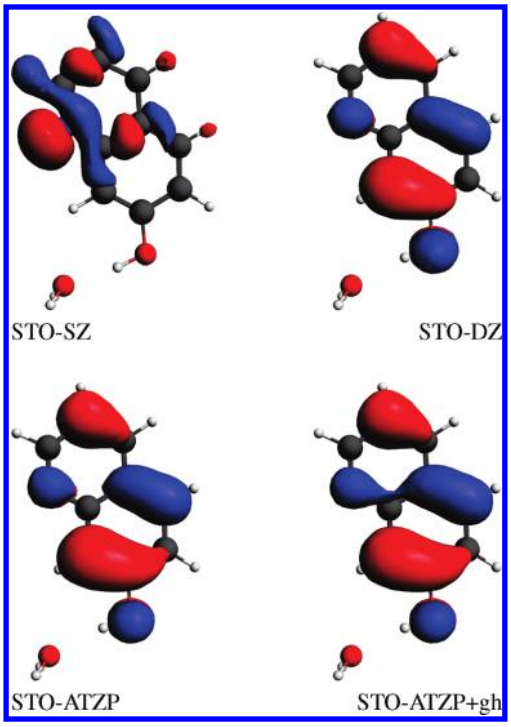

Figure 4. Highest occupied embedded orbital obtained with different basis sets and the full embedding potential: the cis-7HQ-H_2O case.

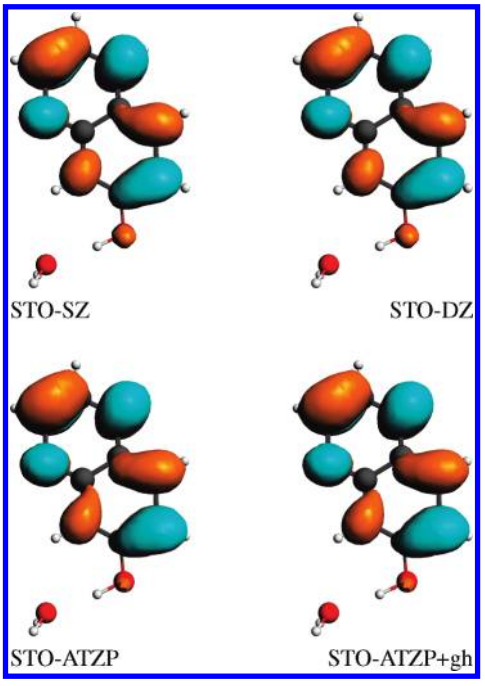

Figure 5. Lowest unoccupied embedded orbital obtained with different basis sets and the full embedding potential: the cis-7HQ-H_2O case.

results are 0.237 and 0.470 eV, respectively), and $\Delta\varepsilon^{LUEO}$) increases from 0.234 to 0.342 eV (the corresponding full potential results are 0.248 and 0.371 eV, respectively). The equivalence of the Coulombic-only and full embedding results is reflected also in the similarity of the shapes of the orbitals involved in the transition (see Figures 2−5). For the complex cis-7HQ···$(H_2O)_2$ (see Table 2), the results obtained with the Coulombic-only and full embedding potentials also agree quite well. The shifts $\Delta\omega$ calculated with the STO-SZ, STO-DZ basis sets are 2285 and −1710 cm^{-1} in the Coulombic-only embedding potential case and the corresponding full-potential results are 2184 and −1703 cm^{-1}, respectively. For the remaining complexes, similar observations can be made concerning the similarity between the full embedding potential and the Coulombic-only embedding potential results obtained with the two smallest basis sets (see Tables 1−8).

Table 10. Experimental Environment-Induced Shifts of the $S_o \rightarrow S_1$ Excitation ($\Delta\omega^{S_o\rightarrow S_1}$ in cm^{-1}) in *cis*-7-Hydroxyquinoline[20]

environment	$\Delta\omega^{S_o\rightarrow S_1}$
H_2O	−590
$(H_2O)_2$	−1637
$(H_2O)_3$	−2060
$(NH_3)_2$	−1715
$(NH_3)_3$	−2030
$(CH_3OH)_2$	−1868
$(CH_3OH)_3$	−2329
$NH_3-H_2O-NH_3$	−1780

The use of the largest basis sets (STO-ATZP and STO-ATZP+gh) reveals, however, a completely different picture concerning the applicability of the Coulombic-only embedding potential. For cis-7HQ···(H_2O) and STO-ATZP, the shift as large as −12999 cm^{-1} is obviously erroneous. It is 1 order of magnitude larger than either the corresponding ab initio reference value of the vertical excitation energy shift (−562 cm^{-1})[34] obtained from high-level wave function based calculations or the shift of the $S_o \rightarrow S_1$ excitation, a closely related experimental quantity to the vertical excitations investigated in the present work amounting −590 cm^{-1} (see Table 10). $\Delta\omega$ calculated with STO-ATZP+gh basis set and the Coulombic-only embedding potential is even worse (−29008 cm^{-1}). These unphysical results for the excitation energies are reflected also in the orbital energies. The situation is similar for cis-7HQ···$(H_2O)_2$. $\Delta\omega$ as large as −8535 cm^{-1} obtained with the Coulombic-only embedding potential and the STO-ATZP basis sets unphysical. Note that the Coulombic-only embedding potential is so erroneous that the convergent solution of eq 5 could not be obtained with the largest basis sets (STO-ATZP and STO-ATZP+gh).

For the remaining six complexes, certain systematic observations can be made concerning the basis set dependence of the Coulombic-only embedding results (see Tables 1 and 8). The agreement between the results obtained with the Coulombic-only and full embedding potential is quantitative for $\Delta\omega$ and at least qualitative for $\Delta\varepsilon^{HOEO}$ and $\Delta\varepsilon^{LUEO}$, only if relatively small basis sets (STO-SZ, STO-DZ) are employed. For larger basis sets, including either diffused functions of the range allowing them to be influenced by the potential near the atoms in the environment or even including basis functions localized there (STO-ATZP and STO-ATZP+gh), the Coulombic-only and full embedding potential results differ qualitatively. The numerical instability of the Coulombic-only embedding is reflected also in the shape of the frontier orbitals (see the change of the shape of HOEO or the change of the localization of LUEO which follows the addition basis sets localized in the water molecule in the cis-7HQ···$(H_2O)_2$ complex shown in

Figures 2 and 3. For other systems, similar global changes in the shape of the frontier orbitals upon addition of the functions into the basis set, which are localized in the environment, occur in the Coulombic-only embedding calculations (data not shown). For all complexes, the lowest excitations evaluated with the Coulombic-only embedding potential and the STO-ATZP or the STO-ATZP+gh basis sets, do not have the $\pi \rightarrow \pi^*$ character. In many cases (cis-7HQ$\cdots$$(H_2O)_3$, cis-7HQ$\cdots$$(CH_3OH)_3$, cis-7HQ$\cdots$$(NH_3-H_2O\text{-}NH_3)$), although the self-consistent but unphysical solutions of eq 5 were obtained, the Davidson procedure[50] for solving the Casida equations of LR-TDDFT[44] failed to converge.

CONCLUSIONS

In all investigated cases, the Coulombic-only embedding potential was shown to lead to numerically unstable excitation energies. Not taking into account the Pauli exclusion principle in the embedding potential leads to erratic results if the size of the basis set increases. Such instabilities are similar to the ones observed in the case of environment-induced shifts in g-tensor reported elsewhere.[36] In the recent literature, however, studies of optical properties applying the Coulombic-only approximation to the embedding potential are reported.[12,13,15−19,51] Usually, rather small basis sets are used, and the dependency of the results is rarely studied in detail. The present results show clearly that, in the presence of the approximated embedding potential, the convergence of the excitation energy shifts with the basis sets is governed by its own rules. Especially, extra caution is required if the Coulombic-only approximation to the embedding potential is applied. The problem of numerical instability of the results obtained with Coulombic-only approximation might be less severe, though, if the exact Coulomb potential considered in the present work is approximated by means of net point charges. We recommend, therefore, that any report of excitation energies obtained from embedding strategy is accompanied by the analysis of the basis set convergence of the calculated shifts. The present study shows also that the numerical stability of the calculated hydrogen-bonding induced shifts can be restored by addition to the Coulombic-only embedding potential, the non-Coulombic component derived from Frozen-Density Embedding Theory[21−25] and approximated using rather simple approximations for its nonadditive kinetic- and exchange-correlation parts. The numerical stability of the shifts obtained with the full FDET embedding potential reflects the variational origin of the potential given in eq 4. We note that the issue of the necessity of taking into account the non-Coulombic components of the embedding operator is reflected in the literature. Typical solutions involve local/nonlocal pseudopotentials or dumping the Coulombic interactions.[4,7−11] Either strategies involve system-dependency of the used approximation for the non-Coulombic part of the embedding operator. The present work indicates that the system-independent embedding potential derived in FDET can be used for the same purpose and leads to convergent results even if the basis set includes orbitals localized on the atoms of the environment. Moreover, the numerical values of the convergent hydrogen-bonding induced shifts in the excitation energy of the lowest transition in *cis*-7-hydroxyquinoline, as shown in our recently published work,[34,35] are in excellent agreement with the benchmark quality shifts derived form Equation-of-Motion Coupled Cluster calculations.

ASSOCIATED CONTENT

Supporting Information. The nuclear geometries of the cis-7HQ molecule and its complexes examined in this study. This material is available free of charge via the Internet at http://pubs.acs.org.

AUTHOR INFORMATION

Corresponding Author
*E-mail: tomasz.wesolowski@unige.ch.

ACKNOWLEDGMENT

This work has been supported by Fonds National Suisse de la Recherche Scientifique (Grant No. 200020-134791/1).

REFERENCES

(1) Warshel, A.; Levitt, M. *J. Mol. Biol.* **1976**, *103*, 227.
(2) Shaik, S.; Cohen, S.; Wang, Y.; Chen, H.; Kumar, D.; Thiel, W. *Chem. Rev.* **2010**, *110*, 949.
(3) Engkvist, O.; Astrand, P. O.; Karlstrom, G. *Chem. Rev.* **2000**, *100*, 4087.
(4) Laio, A.; VandeVondele, J.; Rothlisberger, U. *J. Chem. Phys.* **2002**, *116*, 6941.
(5) Wesolowski, T. A. *J. Am. Chem. Soc.* **2004**, *126*, 11444.
(6) Zbiri, M.; Atanasov, M.; Daul, C.; Garcia-Lastra, J. M.; Wesolowski, T. A. *Chem. Phys. Lett.* **2004**, *397*, 441.
(7) Vaidehi, N.; Wesolowski, T. A.; Warshel, A. *J. Chem. Phys.* **1992**, *97*, 4264.
(8) Valderrama, E.; Wheatley, R. J. *J. Comput. Chem.* **2003**, *24*, 2075.
(9) Arcisauskaite, V.; Kongsted, J.; Hansen, T.; Mikkelsen, K. V. *Chem. Phys. Lett.* **2009**, *470*, 285.
(10) Gordon, M. S.; Freitag, M. A.; Bandyopadhyay, P.; Jensen, J. H.; Kairys, V.; Stevens, W. J. *J. Phys. Chem. A* **2001**, *105*, 295.
(11) DiLabio, G. A.; Hurley, M. M.; Christiansen, P. A. *J. Chem. Phys.* **2002**, *116*, 9578.
(12) Valiev, M.; Kowalski, K. *J. Chem. Phys.* **2006**, *125*, 211101.
(13) Olsen, J. M.; Aidas, K.; Mikkelsen, K. V.; Kongsted, J. *J. Chem. Theory Comput.* **2010**, *6*, 249.
(14) Aidas, K.; Kongsted, J.; Osted, A.; Mikkelsen, K. V. *J. Phys. Chem. A* **2005**, *109*, 8001.
(15) Wanko, M.; Hoffmann, M.; Frauenheim, T.; Elstner, M. *J. Phys. Chem. B* **2008**, *112*, 11462.
(16) Curutchet, C.; Munoz-Losa, A.; Monti, S.; Kongsted, J.; Scholes, G. D.; Mennucci, B. *J. Chem. Theory Comput.* **2009**, *5*, 1838.
(17) Tomasello, G.; Olaso-Gonzalez, G.; Alto, P.; Stenta, M.; Serrano-Andres, L.; Merchan, M.; Orlandi, G.; Bottoni, A.; Garavelli, M. *J. Am. Chem. Soc.* **2009**, *131*, 5172.
(18) Fujimoto, K.; ya Hasegawa, J.; Nakatsuji, H. *Chem. Phys. Lett.* **2008**, *462*, 318.
(19) Nakatani, N.; ya Hasegawa, J.; Nakatsuji, H. *Chem. Phys. Lett.* **2009**, *469*, 191.
(20) Thut, M.; Tanner, C.; Steinlin, A.; Leutwyler, S. *J. Phys. Chem. A* **2008**, *112*, 5566.
(21) Wesolowski, T. A.; Warshel, A. *J. Phys. Chem.* **1993**, *97*, 8050.
(22) Wesołowski, T. A. In *Computational Chemistry: Reviews of Current Trends*; Leszczyński, J., Ed.; World Scientific: Singapore, 2006; pp 1−82.
(23) Wesolowski, T. A. *Phys. Rev. A* **2008**, *77*, 012504.
(24) Pernal, K.; Wesolowski, T. A. *Int. J. Quantum Chem.* **2009**, *109*, 2520.
(25) Lastra, J. M. G.; Kaminski, J. W.; Wesolowski, T. A. *J. Chem. Phys.* **2008**, *129*, 074107.
(26) Zhou, X.; Kaminski, J. W.; Wesolowski, T. A. *Phys. Chem. Chem. Phys.* **2011**, *13*, 10565.

(27) Stefanovich, E. V.; Truong, T. N. *J. Chem. Phys.* **1996**, *104*, 2946.
(28) Govind, N.; Wang, Y. A.; Carter, E. A. *J. Chem. Phys.* **1999**, *110*, 7677.
(29) Neugebauer, J.; Baerends, E. J. *J. Phys. Chem. A* **2006**, *110*, 8786.
(30) Jacob, C. R.; Visscher, L. *J. Chem. Phys.* **2006**, *125*, 194104.
(31) Hodak, M.; Lu, W.; Bernholc, J. *J. Chem. Phys.* **2008**, *128*, 014101.
(32) Gomes, A. S. P.; Jacob, C. R.; Visscher, L. *Phys. Chem. Chem. Phys.* **2008**, *10*, 5353.
(33) Lahav, D.; Kluner, T. *J. Phys.: Condens. Matter* **2007**, *19*, 226001.
(34) Fradelos, G.; Lutz, J. J.; Wesołowski, T. A.; Piecuch, P.; Włoch, M. *J. Chem. Theory Comput.* **2011**, *7*, 1647.
(35) Fradelos, G.; Lutz, J. J.; Wesołowski, T. A.; Piecuch, P.; Włoch, M. In *Progress in Theoretical Chemistry and Physics*; Hoggan, P., Brandas, E., Maruani, J., Delgado-Barrio, G., Piecuch, P., Eds.; Springer: Dordrecht, 2011; Vol. 22.
(36) Fradelos, G.; Wesolowski, T. A. *J. Chem. Theory Comput.* **2011**, *7*, 213.
(37) Neugebauer, J. *J. Chem. Phys.* **2007**, *126*, 134116.
(38) Casida, M. E.; Wesolowski, T. A. *Int. J. Quantum Chem.* **2004**, *96*, 577.
(39) Senatore, G.; Subbaswamy, K. R. *Phys. Rev. B* **1986**, *34*, 5754.
(40) Cortona, P. *Phys. Rev. B* **1991**, *44*, 8454.
(41) Dulak, M.; Wesolowski, T. A. *Int. J. Quantum Chem.* **2005**, *101*, 543.
(42) Köster, A. M.; Flores-Moreno, R.; Geudtner, G.; Goursot, A.; Heine, T.; Reveles, J. U.; Vela, A.; Salahub, D. R. *deMon 2003*; NRC: Canada, 2003; http://www.deMon-software.com/.
(43) Dulak, M.; Kaminski, J.; Wesolowski, T. *J. Chem. Theory Comput.* **2007**, *3*, 735.
(44) Casida, M. E. In *Recent Advances in Density-Functional Methods, Part I*; Chong, D. P., Ed.; World Scientific: Singapore, 1995; pp 155−192.
(45) Neugebauer, J.; Jacob, C. R.; Wesolowski, T. A.; Baerends, E. J. *J. Phys. Chem. A* **2005**, *109*, 7805.
(46) Jacob, C. R.; Neugebauer, J.; Visscher, L. *J. Comput. Chem.* **2008**, *29*, 1011.
(47) *ADF2009*, suite of programs Theoretical Chemistry Department; Vrije Universiteit: Amsterdam, 2009; http://www.scm.com.
(48) Gritsenko, O. V.; Schipper, P. R. T.; Baerends, E. J. *Chem. Phys. Lett.* **1999**, *302*, 199.
(49) Ziesche, P.; Eschrig, H., Eds. Unified theory of exchange and correlation beyond the local density approximation. *Electronic Structure of Solids 1991*; Akademic Verlag: Berlin, 1991; Vol. 10, p 11.
(50) Davidson, E. R. *J. Comput. Phys.* **1975**, *17*, 87.
(51) Murugan, N. A.; Kongsted, J.; Rinkevicius, Z.; Aidas, K.; Mikkelsen, K. V.; Agren, H. *Phys. Chem. Chem. Phys.* **2011**, *13*, 12506.